Response to reviewers comments for AMT-2023-37

Viet Le[1], Hannah Lobo[1], Ewan J. O'Connor[1], and Ville Vakkari[1, 2]

[1]Finnish Meteorological Institute, Helsinki, 00101, Finland
[2]Atmospheric Chemistry Research Group, Chemical Resource Beneficiation, North-West University, Potchefstroom, 2520, South Africa

Correspondence: viet.le@fmi.fi

We would like to thank the reviewers for the constructive comments. Below are the reviewer comments in black text, followed by our responses in blue text. Where applicable, we also provide changes to the manuscript in *blue italics*.

1 Reviewer 2

The manuscript demonstrates the capability of Halo doppler lidars to retrieve the particle linear depolarization ratio (δaerosol)
5   at 1565 nm and investigates the stability of the background noise levels and the performance of the internal polarizer, both of which have to be considered for the retrieval of δaerosol. The retrieved particle linear depolarization ratio is used to perform a seasonal characterization of the suspended aerosols at four different sites of Finland of different environments (e.g. marine, forest, rural, sub artic regions) using four-year lidar measurements from 2016 to 2019. For the seasonal analysis on the δaerosol, a new aerosol identification (AI) algorithm has been developed to separate the aerosol from the cloud layers. The performance
10 of the AI algorithm has been compared against the Cloudnet classification algorithm showing adequate performance on identifying and separating the aerosol layers from the clouds. Moreover, two case studies, one Saharan dust transport event and one pollen from continental areas event, have been selected to be presented in the study while using complimentary data for the air mass origin from FLEXPART model.

To sum up, the manuscript presents new methods and new developments falling within the scope of the journal. It is well-
15 structured and well-written even though I have the feeling that some parts could be further explained and/or discussed in order to be easier to follow for a reader non-relevant to the study. The scientific significance makes the manuscript suitable for publication in AMT, after some minor revisions have been considered from the authors.

We would like to thank the reviewer for their positive evaluation of the manuscript.

Comments:

20 A general comment for the authors is to explain better the difference between δ (is it the volume linear depolarization ratio?) and δ_aerosol (particle linear depol. ratio?) in the text as it might be confusing for the readers

$\delta_{aerosol}$ is an abbreviation for δ of aerosol. To alleviate the confusion, we will replace $\delta_{aerosol}$ with δ of aerosol

Line 53: "... δ_aerosol is measured using Raman lidar (Engelmann et al., 2016; Baars et al., 2016)"

25 The depolarization ratio profile can only be retrieved when a lidar is equipped with depolarization channels, thus from a depolarization lidar (not all Raman lidars have depolarization channels). PollyXTs are Raman and depolarization (and water-vapor) lidar systems. Please rephrase and add also older studies since depolarization in lidar measurements is being used even before 2016 (see for example Sassen, K.: Polarization in Lidar, in Lidar: Range-Resolved Optical Remote Sensing of the Atmosphere, edited by C. Weitkamp, pp. 19–42, Springer New York, New York, NY., 2005)

30 We have rephrased this as:

Typically, δ of aerosol is measured at shorter wavelenghts such as at $355\mu m$, $0.523\mu m$, $0.532\mu m$, $0.694\mu m$, $0.710\mu m$ or $1.064\mu m$ (Murayama et al., 2001; Sassen, 2002; Engelmann et al., 2016; Baars et al., 2016)

Line 124: "...estimate the internal polarizer performance, or bleed-through (Vakkari et al., 2021)". Here you could add a
35 short description about what the bleed-through is, in order to be easier for an independent reader to follow. Then if the reader wants more details, can read the Vakkari et al., 2021.

The bleed-through is defined by Vakkari et al. (2021) as the incomplete extinction in the lidar internal polarizer, which the co-polar signals is leaking into the cross-receiver. This results in a systematic bias in the calculated δ from SNR_{co} and SNR_{cross}.

40 Line 147: "... The mean and standard deviation of δ at the cloud base were then calculated and used to determine the bleed through". Here the authors could also mention that the B term they are using in eq. 3 is the calculated mean value of δ. Moreover, the values of δ at the cloud base do they correspond to an averaged δ inside the range gate that is identified as the cloud base?

Thank you for the suggestion, we have now added to Sect 2.1.2:
45 *The mean and standard deviation of δ at all the cloud bases were then calculated and used to determine the bleed-through for each instrument and to investigate its stability over time.*
And to Sect 2.3:
where B is the estimated bleed-through of each instrument (Table 3).
The values of δ at the cloud base is collected in each individual cloud profile of each instrument. The bleed-through B is the
50 averaged δ of all these profiles of each instrument excluding the tail of the distribution due to mixed-phase cloud or non-ideal sampling of liquid clouds as described in Section 3.1.2.

Lines 159 – 263: These sections are too technical and refer to readers with specific expertise in HALO wind lidar technologies and data handling. Therefore, I would suggest to move these sections in an appendix and maybe lines 170-208 where the
55 steps of AI are described to be moved at the supplement below figure S3. Instead of this too technical description you could add a more qualitative description of the AI and the signal post-processing sections to achieve a smoother transition to section for the investigation of the air mass origins. However, Figure 3 is a good way to demonstrate the results on the target classification from AI and thus could remain in the main text but with further discussion.

Thank you for the comment, we decided to simplify the description of the algorithm in the main part of the manuscript and move some of the technical details to the supplement. Updated Fig. 3 in the manuscript and text replacing lines 170-208 is below.
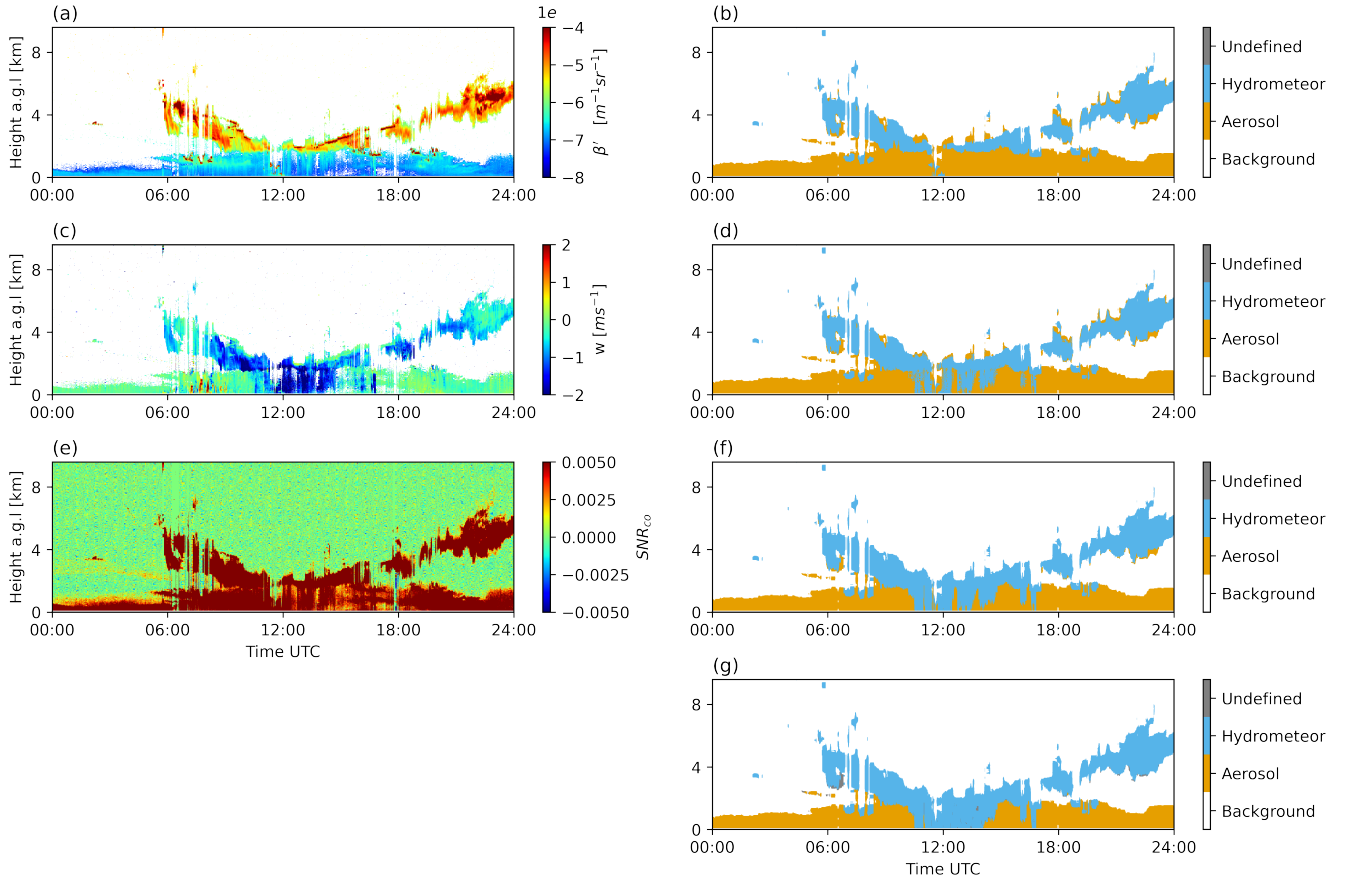
Figure 3. *Atmospheric profiles on 12th of August 2018 at Hyytiälä. The left column displays the measured data where the background noise has been filtered for visualization in [a, c]. a) Attenuated backscatter (β'), c) Vertical velocity (w), e) Signal-to-noise ratio in the co-polar channel (SNR_{co}). The right column displays the steps from the Aerosol Identification algorithm. b) First step, d) Second step, f) Third step, g) Final step, i.e., the final result.*

Figure 3a, 3c, 3e display the measured data from the Doppler lidar in 12th of August 2018 at Hyytiälä. The detail of the Aerosol Identification Algorithm is described in Sect. S3, a brief overview is explained as follows:

1. The first step of the algorithm involves detecting potential hydrometeors and aerosols from background signals based on β' and SNRco. The result of this step is shown in Fig. 3b.

2. The falling hydrometeor detection step involves separating aerosol in downdrafts due to boundary layer mixing from actual precipitation using both β' and w. Regions containing both up- and down- drafts are considered to be characteristic of bound-

ary layer mixing, while a region of continuous downdrafts indicates precipitation. The result of this step is shown in Fig. 3d.

3. Attenuation correction step flagged all observations above clouds and precipitation with their corresponding class since the

70 *signal has been heavily attenuated. The result of this step is shown in Fig. 3f.*

4. In the final step, a fine-tuned aerosol identification process is utilized to improve the aerosol class determination accuracy. First, aerosol clusters are identified using both time and height domain. Then based on the average speed of the aerosol cluster and its connectiveness to the first lidar range gate, it can be classified as either aerosol, hydrometeor or undefined. The final result is shown in Fig. 3g.

75 *The resulting classes are background signal, aerosol, hydrometeor, and undefined. For this algorithm, hydrometeors are defined as cloud (liquid or ice) or precipitation (rain or snow) and do not include aerosol.*

We also simplified the post-processing section, Sect. 2.3

Aerosol is expected to be well-mixed within each aerosol layer, so in order to extract weak aerosol signal and minimize the

80 *random noise, SNR_{co} and SNR_{cross} were averaged for 1 hour.*

As mentioned before, the SNR data in this study have been processed with the background correction algorithm described by Vakkari et al. (2019). Briefly, the noise floor consists of a non-polynomial component, which is obtained from the background checks according to Vakkari et al. (2019) and a polynomial component, which is obtained from a fit to the aerosol- and hydrometeor- free (background) range gates of each SNR_{co} and SNR_{cross} profile (Manninen et al., 2016; Vakkari et al.,

85 *2019). Typically, the linear part of the noise floor is much larger than the 2nd order polynomial component, but for extended averaging (more than 1 hour) it is essential to include in the background correction. An example of this is shown in Fig. 4a demonstrating how this 2nd order polynomial component can greatly affect the δ of aerosol retrieval in aerosol layers with low SNR (Fig. 4d). Previously (Vakkari et al., 2021; Bohlmann et al., 2021), the 2nd order component of the noise floor has been fitted to aerosol- and hydrometeor- free range gates of the SNR profiles based on visual inspection of individual profiles.*

90 *However, given the large number of profiles analysed in this study, this approach is not feasible and thus we have automated the fitting of the 2nd order polynomial. The fitting algorithm is described in detail in the Sect. S2, and the resulting SNR_{co} and SNR_{cross} profiles are shown in Fig. 4b, 4c.*

The attenuated backscatter is calculated from the background-corrected SNR_{co}. Next, aerosol layer(s) are identified using the Aerosol Identification algorithm. Finally, following Vakkari et al. (2021), the bleed-through corrected δ in aerosol regions is

95 *calculated as*

$$\delta = \frac{SNR_{cross} - B \cdot SNR_{co}}{SNR_{co}} \tag{3}$$

where B is the estimated bleed-through of each instrument (Table 3).

The resulting δ is shown in Fig. 4d, and the estimation of its uncertainty is presented in Sect. S2. Additionally, the post-processed δ of aerosol was collected from the whole dataset and compared with the original δ. The result described in Sect. S2 shows

100 *that the post-processing procedure substantially improved the δ of aerosol with low SNR values.*

Line 166: "...2D Kernel manipulation...". What is this 2D-Kernel manipulation? Maybe a description about the basic idea in a sentence along with a reference or link would be helpful. This way the reader can understand that this method is bout image processing.

Thank you for the suggestion, we have now added more clarifications:

105 *The Aerosol Identification algorithm developed here utilizes 2D-kernel manipulation, which is a commonly used approach in image processing (Guo et al., 2022; Li et al., 2013; Perreault and Hébert, 2007), to extract various features from the data and to determine the correct class for each data point. A kernel, also referred to as a filter, template, window or mask (Gonzalez and Woods, 2007) is a small 2-D data array. Mathematical operations, such as median, maximum, Gaussian etc., on all values inside the kernel determine its center value. The kernel is run through each data point one by one, replacing its center value*
110 *with mathematical operations of the neighboring values.*

Lines 299 – 300: "...This is due to the Streamline Pro models were configured to utilize only half of the bandwidth, i.e half the Nyquist velocity...". Could the authors discuss a bit further how the half of bandwidth can affect the noise floor levels? Maybe you could add an extra explanatory sentence along with a reference.

Assuming the noise is thermal noise and is evenly distributed across the frequency spectrum, the noise power follows Johnson-Nyquist noise power equation (Nyquist, 1928; Johnson, 1928):

$$N = kTB,$$

115 where k is the Boltzmann constant, T is the temperature, and B is the bandwidth. So, reducing the bandwidth by half will reduce the noise power by half. The half bandwidth of the Streamline Pro models were configured by the manufacturer.

Line 307: "...Figure 6 displays the time series of δ at liquid cloud base for each instrument in the network." Here the authors could also add that they are using the time series of δ in order to calculate the bleed through (B) and its uncertainty as the mean value and std of δ over time (as you state in lines 318–320).

120 *Figure 6 displays the time series and the distribution of δ at liquid cloud base for each instrument in the network. The time series is used assess the stability of the internal polarizer over time and the distribution is used to calculate the bleed through (B) and its uncertainty. Overall, there is no significant trend in the bleed through of all the instruments.*

Figure 6: Data from the same stations are used in Figures 5 and 6. A suggestion that could help the reader understand faster
125 Figure 6 is to use the same colors for each station of Figure 5 in Figure 6, too.

We agree with your comment, and have modified the plot accordingly
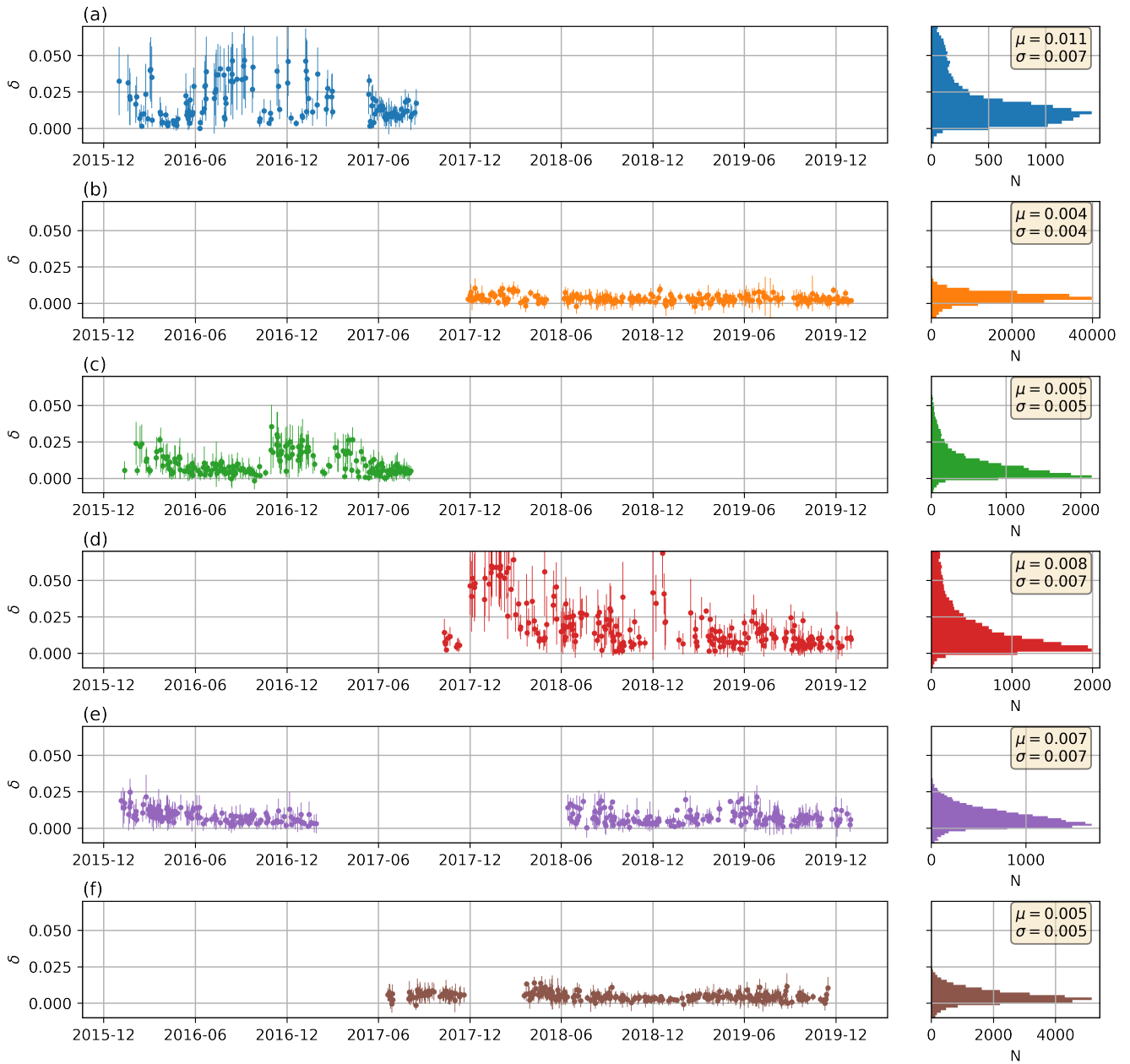
Figure 6. *Time series (left panels) and histogram (right panels) of depolarization ratio (δ) at liquid cloud base in a) Utö-32, b) Utö-32XR, c) Hyytiälä-33, d) Hyytiälä-46, e) Vehmasmäki-53, f) Sodankylä-54. The best estimates of mean (μ) and standard deviation σ of δ at liquid lcoud base in each site are shown in the right panel.*

Section 3.4.1: The effect of relative humidity. In this section the authors mention the diurnal pattern of δ_aerosol and RH below 300 m a.g.l.. How these RH patterns obtained if not measured? Please clarify this also in the caption of Figure 10.

We add clarification in the text

130 *However, as RH profiles are not measured, we investigate the connection between the surface RH at 2 m a.g.l and the δ of aerosol below 300 m a.g.l*

We modified the caption

Diurnal pattern of the particle depolarization ratio of aerosol (δaerosol) from 90m to 300m a.g.l and relative humidity (RH) at 2m a.g.l respectively...

135

References

Baars, H., Kanitz, T., Engelmann, R., Althausen, D., Heese, B., Komppula, M., Preißler, J., Tesche, M., Ansmann, A., Wandinger, U., Lim, J. H., Young Ahn, J., Stachlewska, I. S., Amiridis, V., Marinou, E., Seifert, P., Hofer, J., Skupin, A., Schneider, F., Bohlmann, S., Foth, A., Bley, S., Pfüller, A., Giannakaki, E., Lihavainen, H., Viisanen, Y., Kumar Hooda, R., Pereira, S. N., Bortoli, D., Wagner, F., Mattis, I., Janicka, L., Markowicz, K. M., Achtert, P., Artaxo, P., Pauliquevis, T., Souza, R. A., Prakesh Sharma, V., Gideon Van Zyl, P., Paul Beukes, J., Sun, J., Rohwer, E. G., Deng, R., Mamouri, R. E., and Zamorano, F.: An overview of the first decade of PollyNET: An emerging network of automated Raman-polarization lidars for continuous aerosol profiling, Atmospheric Chemistry and Physics, 16, 5111–5137, https://doi.org/10.5194/acp-16-5111-2016, 2016.

Bohlmann, S., Shang, X., Vakkari, V., Giannakaki, E., Leskinen, A., Lehtinen, K. E., Pätsi, S., and Komppula, M.: Lidar depolarization ratio of atmospheric pollen at multiple wavelengths, Atmospheric Chemistry and Physics, 21, https://doi.org/10.5194/acp-21-7083-2021, 2021.

Engelmann, R., Kanitz, T., Baars, H., Heese, B., Althausen, D., Skupin, A., Wandinger, U., Komppula, M., Stachlewska, I. S., Amiridis, V., Marinou, E., Mattis, I., Linné, H., and Ansmann, A.: The automated multiwavelength Raman polarization and water-vapor lidar PollyXT: The neXT generation, Atmospheric Measurement Techniques, 9, 1767–1784, https://doi.org/10.5194/amt-9-1767-2016, 2016.

Gonzalez, R. C. and Woods, R. E.: Digital Image Processing (3rd Edition), publication Title: Prentice-Hall, Inc. Upper Saddle River, NJ, USA ©2006, 2007.

Guo, S., Wang, G., Han, L., Song, X., and Yang, W.: COVID-19 CT image denoising algorithm based on adaptive threshold and optimized weighted median filter, Biomedical Signal Processing and Control, 75, https://doi.org/10.1016/j.bspc.2022.103552, 2022.

Johnson, J. B.: Thermal Agitation of Electricity in Conductors, Physical Review, 32, 97–109, https://doi.org/10.1103/PhysRev.32.97, publisher: American Physical Society, 1928.

Li, S., Kang, X., and Hu, J.: Image fusion with guided filtering, IEEE Transactions on Image Processing, 22, https://doi.org/10.1109/TIP.2013.2244222, 2013.

Manninen, A. J., O'Connor, E. J., Vakkari, V., and Petäjä, T.: A generalised background correction algorithm for a Halo Doppler lidar and its application to data from Finland, Atmospheric Measurement Techniques, 9, 817–827, https://doi.org/10.5194/amt-9-817-2016, 2016.

Murayama, T., Sugimoto, N., Uno, I., Kinoshita, K., Aoki, K., Hagiwara, N., Liu, Z., Matsui, I., Sakai, T., Shibata, T., Arao, K., Sohn, B. J., Won, J. G., Yoon, S. C., Li, T., Zhou, J., Hu, H., Abo, M., Iokibe, K., Koga, R., and Iwasaka, Y.: Ground-based network observation of Asian dust events of April 1998 in east Asia, Journal of Geophysical Research Atmospheres, 106, https://doi.org/10.1029/2000JD900554, 2001.

Nyquist, H.: Thermal Agitation of Electric Charge in Conductors, Physical Review, 32, 110–113, https://doi.org/10.1103/PhysRev.32.110, publisher: American Physical Society, 1928.

Perreault, S. and Hébert, P.: Median filtering in constant time, IEEE Transactions on Image Processing, 16, https://doi.org/10.1109/TIP.2007.902329, 2007.

Sassen, K.: Indirect climate forcing over the western US from Asian dust storms, Geophysical Research Letters, 29, https://doi.org/10.1029/2001gl014051, 2002.

Vakkari, V., Manninen, A. J., O'Connor, E. J., Schween, J. H., Van Zyl, P. G., and Marinou, E.: A novel post-processing algorithm for Halo Doppler lidars, Atmospheric Measurement Techniques, 12, 839–852, https://doi.org/10.5194/amt-12-839-2019, 2019.

Vakkari, V., Baars, H., Bohlmann, S., Bühl, J., Komppula, M., Mamouri, R. E., and O'connor, E. J.: Aerosol particle depolarization ratio at 1565 nm measured with a Halo Doppler lidar, Atmospheric Chemistry and Physics, 21, https://doi.org/10.5194/acp-21-5807-2021, 2021.